Diffusive and subdiffusive axial transport of granular material in rotating mixers

David Fischer,[1] Tilo Finger,[1] Frank Angenstein,[2] and Ralf Stannarius[1]
[1]*Institute of Experimental Physics, Otto-von-Guericke-University, Universitätsplatz 2, D-39106 Magdeburg, Germany*
[2]*Leibniz Institute for Neurobiology, Brenneckestraße 6, D-39118 Magdeburg, Germany*
(Received 24 June 2009; revised manuscript received 27 August 2009; published 9 December 2009)

The segregation of granular mixtures in rotating cylinders into axial bands is not well understood so far. Abnormal diffusion of the grains has been proposed to play an important role in that process. We measure axial diffusion in binary mixtures, completely embedded in water, by means of nuclear magnetic imaging (magnetic resonance imaging). It is found that the small size particles in a radially segregated structure undergo normal (Fickian) axial diffusion, whereas an initial pulse of the large species shows subdiffusive behavior. An interpretation within a model for the particle dynamics is given. The diffusion of small particles occurs in the axial kernel, whereas particles of the large species migrate on the free surface of the granular bed.

DOI: 10.1103/PhysRevE.80.061302 PACS number(s): 45.70.Mg, 05.65.+b, 83.85.Fg

I. INTRODUCTION

Granular material can behave like a liquid or solid and even like a gas under appropriate experimental conditions. One of the unique, sometimes even counterintuitive properties of granular mixtures is their tendency to separate by size or density under agitation in a wide variety of situations [1–3]. This ubiquitous phenomenon is found both in nature and technological processes. A classical experiment for the study of segregation effects is the horizontally rotating mixer (e.g., [4–25]) in the form of a cylinder, cuboid, sphere, or other. When initially well mixed particles of different sizes are filled into such containers, one observes a radial segregation of the components and the formation of an axially extended core of the smaller-sized particles [5] after few rotations. In many, although not all, mixtures of particles of different sizes this process is followed by an axial banding [11,14]. After this phase, a gradual coarsening of the band structure occurs [10] as a consequence of the redistribution of grains between the individual bands. The physical explanation for the latter processes is not fully clear so far, irrespective of different theoretical models and simulations [8,26–30]. Even though some of these models reproduce the dynamics of axial banding, including oscillatory transients that precede band pattern formation, most of them disregard the true geometry of the experiment, viz., the importance of the core for the particle dynamics. Elperin and Vikhansky [30] assumed that an axial instability of the core is responsible for the observed spatial banding. It seems that the diffusion characteristics of particles in a granular mixture are of crucial importance for the understanding of the segregation dynamics. All models assume that the grains undergo normal (Fickian) diffusion along the container axis. This precondition has been questioned by Khan and Morris [17,18]. Their experiments demonstrate a subdiffusive character of the particle distribution in the axially extended core. The experiments reported by Khan are based on an optical observation of the cylindrical mixer in transmission and an evaluation of particle distribution in the core from the optical transmission intensity and some assumptions of the geometry of the core. Taberlet *et al.* [31–33] in 2006 conducted extensive discrete elements method (DEM) simulations of the corresponding pulse experiments and they reported for their axial propagation normal Fickian diffusion, in agreement with the earlier model assumptions, but in contradiction to Khan's experiments.

Figure 1 shows our experimental geometry. The inner mixer diameter is 36.8 mm, and its length is 662 mm. The mixer is rotated by a stepper motor and observed in transmitted light with a video camera.

We note that the interstitial fluid does not influence the observed structures qualitatively. Fiedor *et al.* [6] demonstrated that similar segregation patterns are formed in dry granulates and in granular mixtures embedded in water. The characteristic ranges of rotation speed are shifted, but the structure formation is comparable in both systems. Our present paper strictly makes predictions for granular mixture in water only, but we assume that for the described experiment such details as the nature of the particle diffusion are not qualitatively influenced by the presence of water as an interstitial medium.

II. EXPERIMENTS

A. Optical experiments

A typical optical experiment is shown in Fig. 2. Bidisperse compositions of glass beads are investigated. The images reflect the evolution of a pulse of small particles (0.55 mm "sil-rock SB" [34]) in large beads (1.5 mm "sil-glass NG" [34]), observed optically in transmission. The mixer was filled with 50% granulate and then filled up with water.

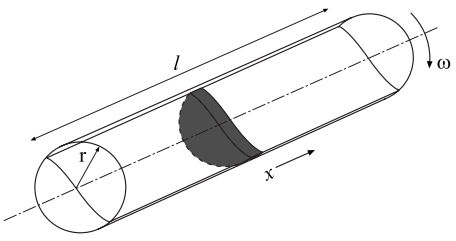

FIG. 1. Sketch of the mixer and definition of geometrical quantities. The dark region represents the initial pulse of diffusing material.

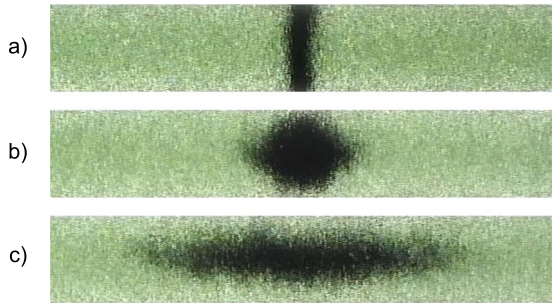

FIG. 2. (Color online) Propagation of a 5 mm pulse of small particles (black) into a bed of large beads. The tube diameter is 36.8 mm, images have been taken (a) before rotation, (b) after 30 s, and (c) 300 s rotation at 30 rpm. The observation direction is normal to the free granulate surface. Using an evaluation procedure as in [17], we obtained in different experiments diffusion exponents α (of the mean-square displacement $\sigma^2 \propto t^\alpha$ of the small beads). The reliability of these results scattering between 0.36 and 0.47 was not convincing.

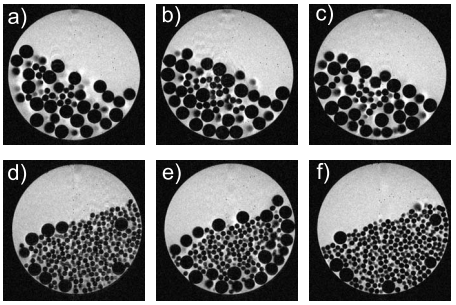

FIG. 3. The top row shows three typical slices of an S pulse after 2.5 rotations, (a) the 0.5-mm-thick slices are taken 5 mm left of the pulse center, (b) in the pulse center, and (c) 5 mm right from it. The bottom row shows three slices of an L pulse after three rotations, taken 10 mm (d) left and (f) right, respectively, (e) from the pulse center.

Alternatively, an immersion liquid (1-methyl-naphthalene plus 28 wt % hexanol) was used in some experiments.

The initial pulse transforms immediately into a core structure which spreads axially with time. Quantitative data analysis of the two-dimensional optical transmission images requires assumptions about the three-dimensional (3D) core structure and compactness. We suggest here a more direct experiment that yields the diffusion properties of grains in the cylindrical mixer. After certain intervals, we stop the rotation and resolve the positions of all beads by use of magnetic resonance imaging (MRI). The exact particle distribution function is evaluated from the particle positions. We obtain the particle statistics at selected time steps and retrieve the diffusion properties. Both the distribution of an initial pulse of small beads in a bed of larger glass beads, and the opposite case are studied. An earlier attempt to study the diffusion properties of granular mixtures in a rotating drum was reported in a pioneering paper by Ristow and Nakagawa [12]. The authors studied a mixture of pharmaceutical pills. The resolution in that experiment was far too low to allow the identification of individual particles so that the concentration profile could not be determined experimentally.

B. MRI experiments

For the MRI experiments, we prepare a single stripe containing a number of $\Sigma=250$ of small beads (2-mm-diameter type "Ornela" [35]) in large beads (4 mm "Sigmund Lindner" type M [36]), designated as S pulse, and in a different experiment a stripe of $\Sigma=100$ large beads (4 mm "Sigmund Lindner" type M) in 1.5 mm small beads ("sil-color" transparent), designated as L pulse. The fill level of the tube is 50%. After the granulate layer is prepared, the tube is completely filled up with water. A rotation speed of 15 rpm was chosen, but the choice of the rotation speed is not critical. NMR experiments are performed in a Bruker BioSpec 47/20 MRI scanner at 200 MHz ^{1}H resonance frequency (4.7 T) using the rapid acquisition with relaxation enhancement (RARE) spin-echo sequence. The inner receiver coil diameter is 7 cm, much larger than the mixer tube. The sensitive volume of the MRI scanner is only 8 cm in axial direction, thus we reconstruct the complete images from a set of three measurements at mutually shifted axial positions, with appropriate overlap. The glass beads appear black on the bright water background in the NMR images (Fig. 3), opposite to MRI experiments with mixtures of water-containing particles, e.g., [11]. A certain technical advantage of our system with interstitial water over MRI measurements of water-containing granulate in air is that we have practically no problems with susceptibility heterogeneities. Such heterogeneities lead, in particular in spectrometers with high magnetic field strengths to local-field inhomogeneities which may limit the experimental resolution.

All individual particle positions are extracted from the 3D image data, and their distribution function $p(x,t)$ is established from histograms with 5 mm box width (Fig. 4). For convenience, we use the number of rotations N of the cylinder as an equivalent of the time t. The effective particle diffusion time is proportional to $t=N/f$ with the rotation frequency f of the cylinder. The maxima of the particle distributions are found from a fit of Gauss functions

$$p(x,N) = p_{\max}(N)\exp\left(-\frac{x^2}{2\sigma^2(N)}\right)$$

to the distributions with the power-law dependence $\sigma \propto N^\alpha$ and $\alpha=1/2$ in normal diffusion. Since the area under each curve is preserved, the distribution maximum should scale with an exponent $\beta=-\alpha$. We find that the maxima $p_{\max}(N)$ (Fig. 5) of the Gauss fits to the discrete particle distribution functions $p(x,N)$ follow a dependence $p_{\max} \propto N^\beta$ with $\beta=-0.52\pm0.03$.

In order to avoid the inaccuracies related to the finite widths of the histogram boxes, we determine the time dependence of σ from cumulative functions $\int_{x_0}^{x} p(x',N)dx'$ with error functions. The lower boundary x_0 is chosen such that $p(x_0,N)=0$. The fits match the experimental data convincingly at all times, see Figs. 4 and 6. The mean-square displacements and maxima of the distribution function as functions of time are in excellent agreement with normal diffusion, $\sigma^2=\langle x^2\rangle=2Dt$ (brackets denote averaging over the

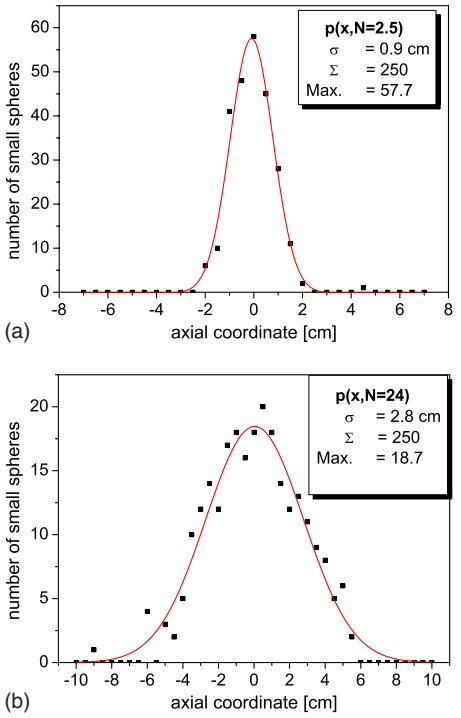

FIG. 4. (Color online) Positions of the small particles in an S pulse (a) after 2.5 rotations of the tube and (b) after 24 rotations. The solid lines are Gauss fit curves.

ensemble). Note that σ determined from the Gauss fit of $p(x,N)$ differs slightly from that of the cumulative fit. We rely on the latter one for the determination of the scaling exponent α.

The repetition of the experiment yielded practically identical statistical results. The mean-square displacement σ^2 is a linear function of the number of revolutions within experimental accuracy. Similarly, the distribution functions of the axial coordinates of diffusing particles are Gaussian and the maximum height of the Gaussian fit curves decays with $p_{\max} \propto N^{-1/2}$ within experimental accuracy, in perfect agreement with normal Fickian diffusion of the small beads in the mixer.

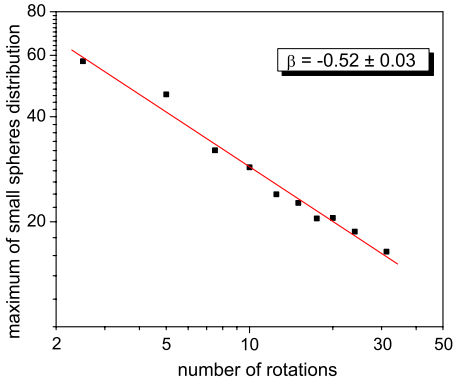

FIG. 5. (Color online) Maximum $p_{\max}(N)$ of the Gauss fit to the discrete particle distribution function $p(x,N)$ (histogram box width 5 mm) vs number of revolutions N. The fit curve represents a dependence $p_{\max} \propto N^{\beta}$ with $\beta = -0.52$.

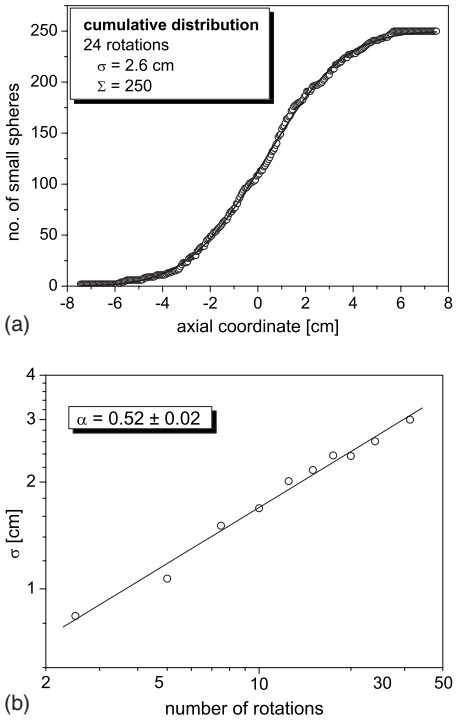

FIG. 6. (a) Cumulative presentation of the particle distribution after 24 revolutions. The solid line is a fit with a Gauss function for $p(x,N)$. (b) Plot of $\sigma(N)$ for the S pulse. The fit represents a potential law $\sigma \propto N^{\alpha}$ with $\alpha = 0.52$.

The second experiment has been performed with $\Sigma = 100$ large beads (same as above) initially forming a narrow stripe (L pulse) surrounded by small beads of 1.5-mm-diameter in the mixer. The evaluation of the MRI data was equivalent to that in the previous experiments. Figure 7 shows the distribution $p(x,N)$ of the initial pulse after six rotations and after 31 rotations, respectively. All distribution functions can be approximated by Gaussians. This encourages us to use integrals of the Gauss shape as fit curves to the cumulative functions $\int_{x_0}^{x} p(x',t)dx'$, as shown exemplarily in Fig. 8(a). The mean-square displacements as functions of time, however, are no longer in agreement with normal diffusion. Instead, as is seen from Fig. 8(b), $\alpha = 0.33$, the mean-square displacement $\langle x^2 \rangle$ is proportional to $N^{0.66}$. Again, a repetition of the experiment reproduced the statistical data with high accuracy. The diffusion of the L pulse is clearly subdiffusive.

Although the distribution functions $p(x,N)$ look rather similar to Gaussians in the latter experiment, they strictly are not. The subdiffusive character ($\alpha < 0.5$) of the particle dynamics implies that the particle distribution is *not* Gaussian. The actual difference between Gaussian model and experiment is systematic but at the limits of resolution [it is hardly acknowledged in Fig. 8(a)]. It becomes evident when the difference between the Gaussian model and the experiment is plotted (see Fig. 9). The plot suggests that diffusion is somewhat faster in the high concentration regions near the initial pulse position and slower in the lateral low concentration regions. In the particle distribution function, this leads to a lower gradient of $p(x)$ than for a Gaussian near the maximum of the distribution and to steeper tails. In the cumulative

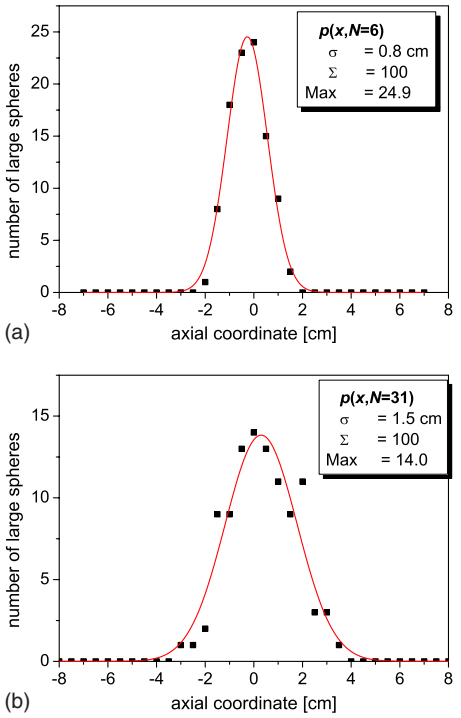

FIG. 7. (Color online) Positions of the large particles in an L pulse (a) after six rotations of the tube and (b) after 31 rotations. The solid lines are Gauss curves.

distribution, the integral of $p(x)$, one consequently expects systematic deviations such as qualitatively sketched by the dashed line in Fig. 9.

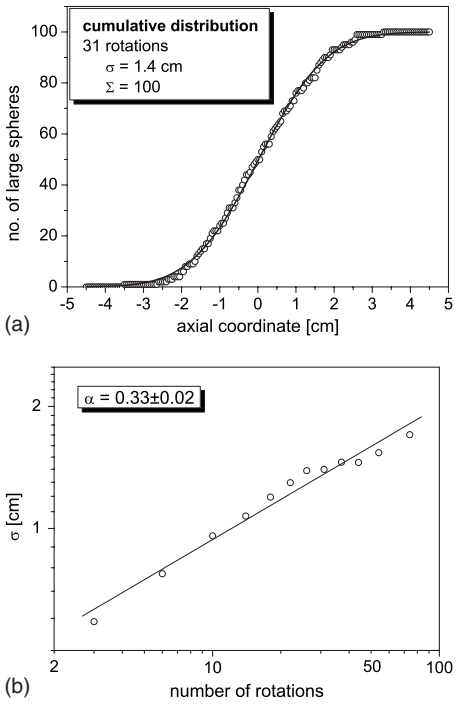

FIG. 8. (a) Cumulative presentation of the particle distribution after 31 mixer rotations. (b) Plot of $\sigma(N)$ as a function of the number of revolutions N for the L pulse. The fit represents a potential law $\sigma \propto N^{\alpha}$ with $\alpha=0.33$.

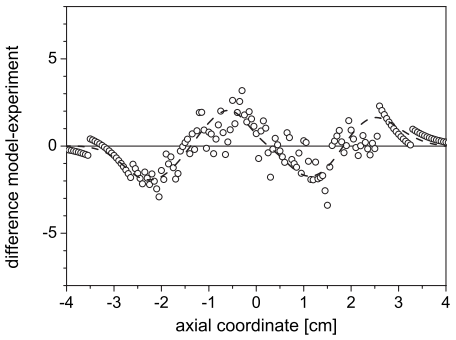

FIG. 9. Difference between the actual cumulative particle distribution [Fig. 8(a)] and the Gaussian model for the L pulse after 31 rotations. The dashed line guides the eye only.

III. DIFFUSION MODEL FOR LARGE BEAD PULSES

From the measured exponent $\alpha \approx 0.33$ and the profile of Fig. 9, it seems natural to assume a concentration-dependent diffusion for an interpretation of the subdiffusive character of the large beads pulse. A concentration-dependent diffusion constant $D(p)$ in the (one-dimensional) diffusion equation

$$\frac{\partial p}{\partial t} = \frac{\partial}{\partial x}\left(D(p)\frac{\partial p}{\partial x}\right)$$

renders this type of equation in general analytically unsolvable, with few exceptions (e.g., [37–39]). For example, the assumption of $D=D_0(p/p_0)^n$ yields a scaling of σ with $t^{1/(n+2)}$ [39]. Our experimental data are not sufficient to allow the extraction of the actual $D(p)$ dependence, but it is obvious that there is a uniform trend $dD/dp>0$ in our L-pulse system. This trend can be understood from a physical point of view. Figure 3, bottom shows that the large particles are on the free surface or rotate attached to the glass wall. The dynamics of their redistribution occurs essentially while they slide down the free surface. At low local concentrations of those particles on the surface, they slide straight down the slope and their lateral diffusion is weak, whereas at larger concentrations, the large particles interact with each other on the slope via collisions. Such collisions increase a stochastic lateral motion and lead to a higher diffusion coefficient. This explains the trend of the systematic deviations from normal diffusion reflected in the measured exponent α, and the subdiffusive character of the spreading of the L pulse.

IV. SUMMARY

We have demonstrated by magnetic resonance imaging investigations that in a granular mixture contained in a rotating cylindrical container, the small particles undergo normal diffusion. A comparison with our optical investigations shows that the data obtained from the optical experiment are not reliable enough to extract the scaling exponent. This may be partially attributed to problems with the projection technique. There are two major problems with the optical experiments. The first one is the relation between the composition of the mixture and the optical transmission intensity, which cannot be established with the desired accuracy. The second

problem is connected with the assumptions about the three-dimensional shape of the segregated core, which cannot be verified with this method.

The MRI experiments are much more reliable, and they provide a powerful tool to study granular dynamics. We conclude that the small particles dynamics can be described with models assuming normal diffusion. This does not necessarily mean that this result can be generalized, in particular in view of the systems studied by Khan and Morris [17]. Rather, it demonstrates that the conditions for diffusion in the rotating cylinder are more complex [18] and may depend on specific details of mixtures and geometries. Our MRI experiments are in qualitative agreement with DEM simulations published recently [32]. Taberlet and Richard discussed in their paper the discrepancies between their work and the experimental data in Ref. [17]. They propose different explanations: the force model in the simulations might be inappropriate, there could be problems with the experimental data evaluation, in particular the projection technique in the optical experiment, and the reason could be physical differences in the two investigated systems (particle and mixer diameters and particle shapes). The clear result of the MRI experiment is that in our investigated system a pulse of small beads spreads axially by normal diffusion.

Large particles that were initially contained in a narrow stripe clearly show subdiffusive dynamics. This indicates that the mechanism of the particle redistribution is essentially different. Physically, this can be explained by a concentration-dependent diffusion coefficient, in connection with the experimental observation that the axial dynamics of the large particles in that case occurs exclusively on the surface of the granular bed. It is clear that this phenomenon should be observable only when there is a sufficient concentration gradient of large particles on the granular bed surface. When the amount of large beads is large enough, the diffusion is expected to be Fickian, like in the case of a small pulse of small-sized particles.

ACKNOWLEDGMENTS

Support by J. Stadler and L. Naji in the MRI experiments are acknowledged. The authors thank Z. Khan and S. Morris for useful and stimulating discussions.

[1] G. H. Ristow, *Pattern Formation in Granular Material* (Springer, Berlin, 2000).
[2] L. P. Kadanoff, Rev. Mod. Phys. **71**, 435 (1999).
[3] J. M. Ottino and D. V. Khakhar, Annu. Rev. Fluid Mech. **32**, 55 (2000).
[4] Y. Oyama, Sci. Pap. Inst. Phys. Chem. Res. (Jpn.) **6**, 600 (1939); **37**, 17 (1940).
[5] E. Clement, J. Rajchenbach, and J. Duran, Europhys. Lett. **30**, 7 (1995); F. Cantelaube and D. Bideau, *ibid.* **30**, 133 (1995).
[6] S. J. Fiedor and J. M. Ottino, Phys. Rev. Lett. **91**, 244301 (2003).
[7] T. Arndt, T. Siegmann-Hegerfeld, S. J. Fiedor, J. M. Ottino, and R. M. Lueptow, Phys. Rev. E **71**, 011306 (2005).
[8] O. Zik, D. Levine, S. G. Lipson, S. Shtrikman, and J. Stavans, Phys. Rev. Lett. **73**, 644 (1994).
[9] M. Nakagawa, S. A. Altobelli, C. Caprihan, E. Fukushima, and E.-K. Jeong, Exp. Fluids **16**, 54 (1993).
[10] M. Nakagawa, Chem. Eng. Sci. **49**, 2540 (1994).
[11] M. Nakagawa, S. A. Altobelli, C. Caprihan, and E. Fukushima, Chem. Eng. Sci. **52**, 4423 (1997).
[12] G. H. Ristow and M. Nakagawa, Phys. Rev. E **59**, 2044 (1999).
[13] K. M. Hill and J. Kakalios, Phys. Rev. E **49**, R3610 (1994); **52**, 4393 (1995).
[14] K. M. Hill, A. Caprihan, and J. Kakalios, Phys. Rev. Lett. **78**, 50 (1997); Phys. Rev. E **56**, 4386 (1997).
[15] K. M. Hill, N. Jain, and J. M. Ottino, Phys. Rev. E **64**, 011302 (2001).
[16] N. Jain, D. V. Khakhar, R. M. Lueptow, and J. M. Ottino, Phys. Rev. Lett. **86**, 3771 (2001).
[17] Z. S. Khan and S. W. Morris, Phys. Rev. Lett. **94**, 048002 (2005).
[18] Z. Khan, PhD thesis, University of Toronto, Toronto, 2006.
[19] A. Alexander, F. J. Muzzio, and T. Shinbrot, Granular Matter **5**, 171 (2004).
[20] L. Prigozhin and H. Kalman, Phys. Rev. E **57**, 2073 (1998).
[21] S. J. Fiedor, P. Umbanhowar, and J. M. Ottino, Phys. Rev. E **73**, 041303 (2006).
[22] T. Finger, A. Voigt, J. Stadler, H. G. Niessen, L. Naji, and R. Stannarius, Phys. Rev. E **74**, 031312 (2006); T. Finger and R. Stannarius, *ibid.* **75**, 031308 (2007).
[23] L. Naji and R. Stannarius, Phys. Rev. E **79**, 031307 (2009).
[24] P. Chen, B. J. Lochman, J. M. Ottino, and R. M. Lueptow, Phys. Rev. Lett. **102**, 148001 (2009).
[25] G. Juarez, J. M. Ottino, and R. M. Lueptow, Phys. Rev. E **78**, 031306 (2008).
[26] D. C. Rapaport, Phys. Rev. E **65**, 061306 (2002).
[27] B. Levitan, Phys. Rev. E **58**, 2061 (1998).
[28] D. Levine, Chaos **9**, 573 (1999).
[29] I. S. Aranson and L. S. Tsimring, Phys. Rev. Lett. **82**, 4643 (1999); I. S. Aranson, L. S. Tsimring, and V. M. Vinokur, Phys. Rev. E **60**, 1975 (1999).
[30] T. Elperin and A. Vikhansky, Phys. Rev. E **60**, 1946 (1999).
[31] N. Taberlet, W. Losert, and P. Richard, Europhys. Lett. **68**, 522 (2004).
[32] N. Taberlet and P. Richard, Phys. Rev. E **73**, 041301 (2006).
[33] N. Taberlet, M. Newey, P. Richard and W. Losert, J. Stat. Mech.: Theory Exp. **2006**, P07013 (2006).
[34] Sil-trade, D-02956 Rietschen, Germany.
[35] Jablonex group as, Division glass, CH-46861 Desna v J.h., Czech Republic.
[36] Sigmund Lindner GmbH, D-95485 Warmensteinbach, Germany.
[37] H. Fujita, Text. Res. J. **22**, 757 (1952); **22**, 823 (1952); **24**, 234 (1954).
[38] J. R. Philip, Nature (London) **185**, 233 (1960).
[39] R. E. Pattle, Q. J. Mech. Appl. Math. **12**, 407 (1959).